# Supplementary Material for

## Large Language Models for Material Property Predictions: elastic constant tensor prediction and materials design

Siyu Liu, Tongqi Wen, Beilin Ye, Zhuoyuan Li, Han Liu, Yang Ren, and David J. Srolovitz

# 1 Supplementary Notes

## 1.1 Model parameter settings

**ElaTBot-DFT training settings**:

- Pre-trained model: Llama2-7b
- learning rate: 5e-05
- train batch size: 3
- eval batch size: 3
- seed: 42
- distributed type: multi-GPU
- num devices: 4
- total train batch size: 12
- total eval batch size: 12
- optimizer: Adam with betas=(0.9,0.999) and epsilon=1e-08
- lr scheduler type: cosine
- lr scheduler warmup steps: 20
- num epochs: 5.0
- mixed precision training: Native AMP
- lora alpha: 16
- lora r: 8
- lora target modules: all

* Also applicable to other prompt types.

**Darwin training settings**:

- Pre-trained model: Darwin-7b
- learning rate: 5e-05
- train batch size: 3
- eval batch size: 3
- seed: 42
- distributed type: multi-GPU
- num devices: 4
- total train batch size: 12
- total eval batch size: 12
- optimizer: Adam with betas=(0.9,0.999) and epsilon=1e-08
- lr scheduler type: cosine
- lr scheduler warmup steps: 20

- num epochs: 5.0
- mixed precision training: Native AMP
- lora alpha: 16
- lora r: 8
- lora target modules: all

**Random forest model training settings**:

- criterion: squared error
- bootstrap: True
- random state: 42

**MatTen model training settings**:

- average num neighbors: auto
- conv layer irreps: 32x0o+32x0e + 16x1o+16x1e + 4x2o+4x2e + 2x3o+2x3e + 2x4e
- conv to output hidden irreps out: 16x0e + 2x2e + 4e
- invariant layers: 2
- invariant neurons: 32
- irreps edge sh: 0e + 1o + 2e + 3o + 4e
- nonlinearity type: gate
- normalization: batch
- num layers: 3
- num radial basis: 8
- output format: irreps
- output formula: ijkl=jikl=klij
- radial basis end: 5.0
- radial basis start: 0.0
- radial basis type: bessel
- reduce: mean
- resnet: true
- species embedding dim: 16
- average num neighbors: 31.68900489807129
- lr scheduler hparams:
  - class path: torch.optim.lr_scheduler.ReduceLROnPlateau
  - init args:
  - factor: 0.5
  - mode: min
  - patience: 50
  - verbose: true

- optimizer hparams:
  - class path: torch.optim.Adam
  - init lr: 0.01
  - init weight decay: 1.0e-05
- epoch: 200
- batch size: 12

**ElaTBot training settings**:

- Pre-trained model: Llama2-7b
- learning rate: 5e-05
- train batch size: 3
- eval batch size: 3
- seed: 42
- distributed type: multi-GPU
- num devices: 4
- total train batch size: 12
- total eval batch size: 12
- optimizer: Adam with betas=(0.9,0.999) and epsilon=1e-08
- lr scheduler type: cosine
- lr scheduler warmup steps: 20
- num epochs: 5.0
- mixed precision training: Native AMP
- lora alpha: 16
- lora r: 8
- lora target modules: all

## 1.2 Computational efficiency of ElaTBot

We compare the computational cost of training ElaTBot-DFT and MatTen using identical training sets; ElaTBot-DFT required 4 hours and 55 minutes on 4 V100 GPUs and training MatTen required 9 hours and 52 minutes on a single V100 GPU. Although ElaTBot-DFT's training required approximately twice the resources of MatTen, ElaTBot-DFT has $\sim$ 20 M trainable parameters compared to MatTen's $\sim$ 3.5 M. In other words, ElaTBot-DFT has 5.7 times more trainable parameters than MatTen but only requires twice the training time. More specifically, training ElaTBoT on an 4 NVIDIA V100 GPUs required 20 hours and training ElaTBoT-required 5 hours on the same system. From a usage perspective, predicting the elastic constant tensor for a single material requires 2 seconds on 4 V100 GPUs, a cost which is reasonable by nearly any accounting. Furthermore, it can integrate additional functionalities beyond elastic constant prediction, which we believe makes it a valuable contribution.

## 1.3 Prompt development

We developed our prompts based on experience with composition based textual prompts and combined it with textual prompts related to crystal structure. We then investigated how the combined approach worked compared with the individual prompt approaches via ablation tests. This was demonstrated in Fig. 2 of our manuscript and Supplementary Tables S1-S2. These tests confirm that the final ElaTBot-DFT prompt (combining both materials composition and crystal structure information) yields superior performance compared to using either information type independently. Ablation tests represent prompt line comparisons/validation. This same ablation-based approach is extendable to further prompt engineering – as other textual features are considered.

# 2 Supplementary Figures

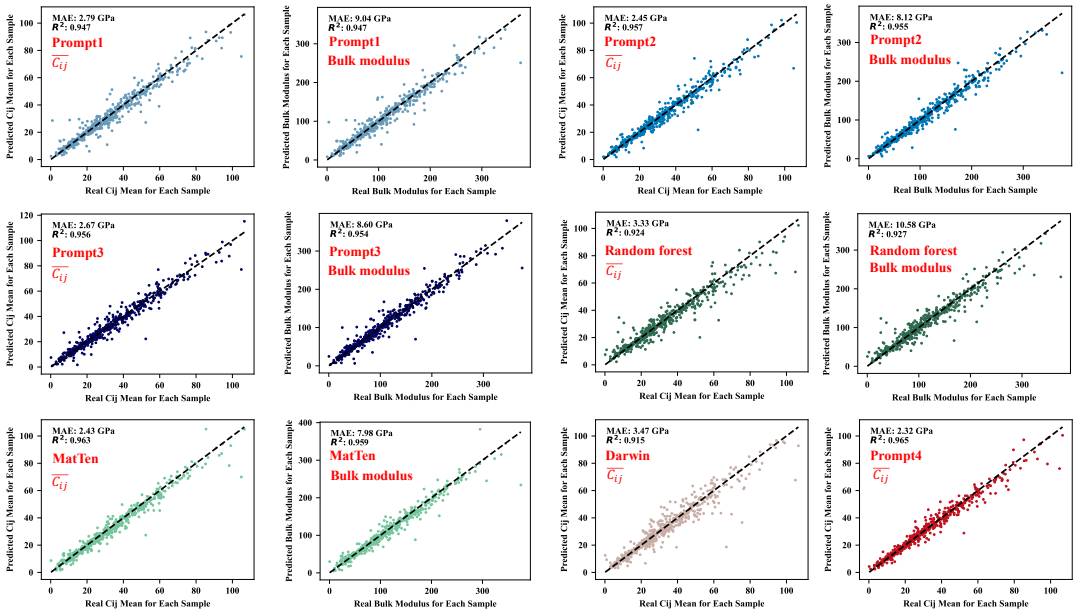


FIG. S1. Model performance comparison in elastic constant tensor and bulk modulus prediction. Performance of various models and prompt types in generating elastic constant tensors and calculating bulk modulus (derived from elastic constant tensors) on a shared test set, following training on a standardized training set.

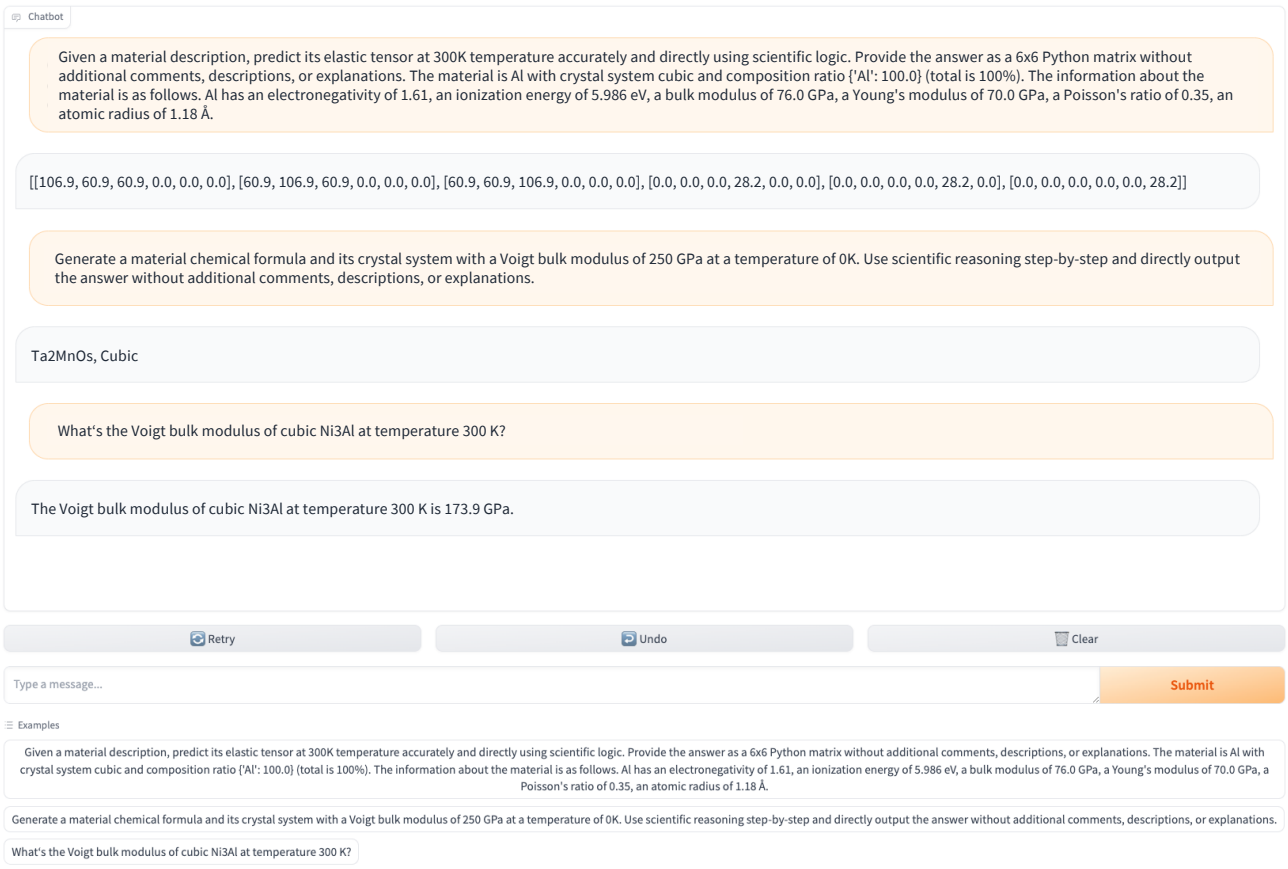


FIG. S2. Chat Agent Interface of ElaTBot. The ElaTBot user interface enables interactive queries for materials prediction and generation. The default training prompt is included to assist users, with options for modification based on specific needs.

As a materials expert, please review the list of materials provided and select those with a bulk modulus comparable to that of bone, suitable for bone implantation and dental restoration. The selected materials should exhibit excellent corrosion resistance and biocompatibility, with a corrosion rate of less than 0.3 mm/year and an LD50 value of less than 3 g/kg body weight. Please respond in JSON list format. Each JSON entry should include the potential materials and the rationale for their suitability in orthopedic applications.

```
['Pr3In', 'NaAl3', 'BaSb3', 'Y3Al', 'La3InB', 'LiGa', 'Sr3SnO', 'Pm2MgTl', 'NaTl2GaF6', 'SmDyMg2', 'NaSmHg2', 'TbMg', 'TmMg3', 'Ca2N', 'LiCuS',
'Li2AgAu', 'SrS', 'LiMg2Hg', 'Li3Pt', 'BaCuBi', 'Pm2MgGa', 'Sr2H6Ru', 'LaPb3', 'Na2CO3', 'Li3AlF6', 'Ba3SnO', 'MgSc', 'Pr3Sn', 'Sr3AsN', 'Tm3TlC',
'Sm2MgTl', 'La2ZnAg', 'SrAl2', 'Tm3AlC', 'La3Al', 'YErMg2', 'Mg3Cu', 'Pr2TlCd', 'Li2AgPb', 'Li2CePb', 'Nd2MgTl', 'Mg6ZrC', 'BaGe2', 'Ca6In2NF',
'LiCdAs', 'Ba(MgAs)2', 'Sr3(AlSi)2', 'Sr2SbAu', 'Ba2H6Ru', 'Li2InAg', 'BaZnGe', 'CaSnHg', 'Li2S', 'CaCdSn', 'Mg3Cd', 'YTmMg2', 'BaAlGe', 'La3Ga',
'TmTl3', 'Pr3Al', 'SrSnHg', 'Ba3(AlGe)2', 'CaCdHg2', 'Li2PmPb', 'BaZnSi', 'Na2O', 'CaPmHg2', 'NdLuMg2', 'Tb3TlC', 'Pr2MgTl', 'Nd2MgIn', 'LiTbSe2',
'CaPmZn2', 'Sr3(AlGe)2', 'CaZnSn', 'Sr(MnSb)2', 'SrAlGe', 'NaAlSi', 'SmLuMg2', 'CaMg6W', 'Pm2MgAl', 'Mg13Al14', 'LaIn', 'Na2O2', 'Mg3Tl',
'Sr3BiN', 'Ca(MnSb)2', 'BaSbAu', 'MgCd', 'Li3Al', 'NaPmHg2', 'TbMg3', 'Mg3Mn', 'Li3SbS4', 'Mg6SiB', 'NaSnP', 'Ba3N2', 'Li3Ga', 'LiGa3', 'SrCuBi',
'NdTm3', 'La2ZnIn', 'YMgTl2', 'Li2GaAg', 'Pr2MgIn', 'Ba2Cu(OF)2', 'TbTmMg2', 'SrCdPt2', 'Li2CeAu', 'PmMgTl2', 'Li3GaN', 'Nd2TlCd', 'LaMgCd2',
'La2AgHg', 'SrZnGe', 'SrCdSi', 'Ca2SiHg', 'Ba2PdAuO6', 'Pr2CdIn', 'SrCdPt', 'TbMgTl2', 'NdMgCd2', 'Sr(AlGe)2', 'Tb3In', 'PrErTl2', 'Tb2MgIn',
'Ca6Si2NF', 'YTm3', 'Mg3Zn', 'Y2MgTl', 'Pm2MgIn', 'CaZn2Sn', 'CaSn2', 'Y2MgIn', 'LiMgSn', 'Sm2MgIn', 'SrPmHg2', 'NaHoHg2', 'SmTmMg2',
'SrCdAu2', 'NaCdP', 'Li3InN', 'Tb2MgTl', 'Ba2MgN2', 'Pr2ZnIn', 'YTl', 'Tm2Mg', 'TbLuMg2', 'LaMgHg2', 'NdSmTl2', 'PmMgCd2']
```

```
[{'material': 'Y3Al', 'rationale': 'Y3Al has a bulk modulus that aligns well with that of bone, providing similar mechanical properties. It is also noted for
its excellent corrosion resistance, making it suitable for bone implantation.'}, {'material': 'LiGa', 'rationale': 'LiGa exhibits good biocompatibility and a
bulk modulus that is comparable to bone. Its low corrosion rate makes it an attractive candidate for dental restoration and orthopedic applications.'},
{'material': 'La3InB', 'rationale': 'La3InB shows favorable mechanical properties with a bulk modulus close to bone. Its corrosion resistance and low
toxicity levels support its use in medical applications.'}, {'material': 'Pr3In', 'rationale': 'Pr3In has a bulk modulus similar to bone, providing the
necessary mechanical support. Additionally, it has demonstrated good corrosion resistance, essential for orthopedic implants.'}, {'material': 'TmMg3',
'rationale': 'With a bulk modulus comparable to that of bone, TmMg3 is a strong candidate for bone implants. It also has excellent corrosion resistance
and biocompatibility.'}, {'material': 'Sr3SnO', 'rationale': "Sr3SnO's bulk modulus aligns well with bone properties, and it demonstrates outstanding
corrosion resistance, making it suitable for both bone implantation and dental restoration."}, {'material': 'Li3Ga', 'rationale': 'Li3Ga exhibits
biocompatibility and a bulk modulus that is close to that of bone, making it ideal for applications in orthopedic devices.'}, {'material': 'Ca2N', 'rationale':
'Ca2N possesses a bulk modulus similar to bone and has shown good biocompatibility, making it a potential candidate for dental restoration.'},
{'material': 'LiCuS', 'rationale': 'LiCuS has a comparable bulk modulus to bone and good corrosion resistance, which are essential for orthopedic
applications.'}, {'material': 'Li3Pt', 'rationale': 'Li3Pt shows mechanical properties and bulk modulus similar to bone, alongside acceptable corrosion
resistance, suitable for use in implants.'}, {'material': 'Na2CO3', 'rationale': 'Na2CO3 is biocompatible and has a bulk modulus near that of bone, making
it suitable for dental applications.'}, {'material': 'SrAl2', 'rationale': 'SrAl2 demonstrates a bulk modulus comparable to that of bone, along with good
corrosion resistance, making it suitable for orthopedic applications.'}, {'material': 'La3Al', 'rationale': 'La3Al exhibits similar mechanical properties to
bone and shows promising corrosion resistance, making it suitable for dental and orthopedic use.'}, {'material': 'BaCuBi', 'rationale': 'BaCuBi has a bulk
modulus comparable to bone, along with good biocompatibility and corrosion resistance for medical applications.'}]
```

FIG. S3. Conversational records with GPT-4o for bone-Like orthopedic materials. Documentation of interactions with GPT-4o to identify materials with properties suitable for orthopedic applications, resembling bone-like characteristics. The material list includes deduplicated compositions generated by ElaTBot.

As a materials expert, please screen from the provided materials list and identify potential low shear modulus materials suitable for the exoskeletons of soft robots. Please respond in JSON list format. Each JSON should include the potential materials and the reasons why they might meet the requirements.

```
['TiRe2W', 'Ti2OsRu', 'Ti2ReOs', 'TiTc2W', 'NbSiTc2', 'Mn3AlC', 'SiC', 'Ti2TcOs', 'V3Rh', 'V2ReRu', 'VRu', 'TaCr2', 'TiN', 'Mn2CoSi',
'TaAlOs2', 'TaTiTc2', 'V2CrRu', 'Nb3Ir', 'V3B4', 'TiSiOs2', 'NbCr3', 'TiVTc2', 'NbRu', 'TaRu3', 'MnV2Os', 'Cr3Pt', 'BeCo2Si', 'TaRh3',
'Ta2OsW', 'BeVOs2', 'TiO', 'Ta2ReMo', 'TaTiRe2', 'Be2C', 'Ta2MnOs', 'Mn2AlRe', 'TiTc2Sb', 'MnV', 'TiRe', 'VPt3', 'Mn3Si', 'TaTiOs2',
'BeVRu2', 'NbRu3', 'Be2IrPd', 'V3Ru', 'Cr3Ru', 'Nb3Ru', 'Cr3Ni', 'Nb3Os', 'VPt', 'TiOs', 'Ta2MoOs', 'TiRu3', 'Mn3GaN', 'MnN',
'Cr3Os', 'BeSiRu2', 'TiSiTc2', 'BeRu2W', 'Nb4C3', 'Si3N4', 'TaRu', 'Ta2VOs', 'V3Os', 'Mn3Pt', 'TaVRu2', 'Si2Mo3', 'TiVOs2',
'Mn2VN', 'Mn2SiW', 'BeRh2W', 'Mn3V', 'Mn3Nb', 'Ta2OsPd', 'Mn2NbW', 'V3C', 'Mn2VRu', 'Cr3C']
```

```
[{'material': 'Mn3AlC', 'reason': 'Manganese-based compounds with low shear modulus, potentially due to structural softness;
commonly explored in soft robotics for flexible designs.'}, {'material': 'TiO', 'reason': 'Titanium oxides are known for their relatively
low shear modulus, making them suitable for applications that require flexibility and compliance, ideal for soft exoskeletons.'},
{'material': 'TiSiOs2', 'reason': 'Titanium-silicon-based materials can offer low shear properties and possess flexibility while being
robust enough for soft robotic applications.'}, {'material': 'MnN', 'reason': 'Manganese nitrides can exhibit a low shear modulus,
making them suitable for applications needing flexible, adaptable materials in dynamic environments.'}, {'material': 'BeCo2Si',
'reason': 'Beryllium-cobalt-silicon materials often have low shear modulus and are lightweight, making them well-suited for soft
robotic exoskeletons that require both flexibility and minimal weight.'}, {'material': 'Be2C', 'reason': 'Beryllium carbide is known for
its low shear modulus, which can provide flexibility required in soft robotics while maintaining structural integrity.'}, {'material':
'Mn3Si', 'reason': 'Manganese-silicon compounds may offer low shear modulus properties, providing the necessary flexibility for soft
robotic applications, and are generally lightweight.'}, {'material': 'Cr3Ni', 'reason': 'Chromium-nickel alloys can have a low shear
modulus depending on the specific alloy structure, potentially suitable for applications in flexible exoskeleton components.'},
{'material': 'Mn3GaN', 'reason': 'Manganese gallium nitride has been explored for its low shear modulus, which could be
advantageous in soft robotics requiring flexibility and compliance.'}, {'material': 'V3Ru', 'reason': 'Vanadium-ruthenium materials can
exhibit low shear modulus properties, making them potentially suitable for exoskeleton designs requiring flexibility in soft robotic
applications.'}]
```

FIG. S4. Conversational records with GPT-4o for low shear modulus material discovery. Documentation of interactions with GPT-4o to identify low shear modulus materials that could be used in the exoskeletons of soft robots. The material list provided consists of deduplicated compositions generated by ElaTBot. ElaTBot is responsible for generating materials with corresponding bulk moduli, while GPT-4o is responsible for screening materials with low shear moduli.

You are a materials expert. Please filter materials from the list provided below that may have better corrosion resistance performance than stainless steel and can be used in saltwater environments. Answer in JSON list format. Each JSON contains possible materials and reasons why they may be corrosion-resistant and able to be used in saltwater environments.

```
['NbInO4', 'TbB2', 'Al3Pt2', 'AlPd', 'Ti3AlC2', 'Zr2TcPd', 'YPt2', 'Hf3(Cu2Ge)2', 'DyB6', 'Tb(PRu)2', 'Ti3Pt', 'TiSbRu', 'HfAlNi2', 'SmPt3', 'Y(CoB)2', 'ZnRhO3', 'TiPd', 'Ti2MnNi', 'ScRh', 'YB6', 'AlSnO3', 'MgZrIr2', 'ScCo2Sn', 'TiFe2Sn', 'TiAlPd2', 'LuN', 'ScPt', 'HfGaCo2', 'Ti2ZnRe', 'MgNi3C', 'ScPd3C', 'NdB6', 'ScGaRh2', 'Ti2TcPd', 'TiAlNi2', 'YRh2', 'DyRh2', 'LiAlRh2', 'Sm(PRu)2', 'Nb2SnC', 'AlVNi2', 'MgSnO3', 'Al2Fe3Si4', 'LiZrRh2', 'TiFeTe', 'Ti3Os', 'Hf2CoTe', 'Ti2TcNi', 'TmPt3', 'TiAlPt', 'LiGeRh2', 'TiSnO3', 'ScInPt2', 'TiNi', 'GaFe3', 'Nd(PRu)2', 'NdBRh3', 'HfP', 'HfNi2Sn', 'ScAlPt2', 'ZnNi2Ge', 'TmNi5', 'ScSnRu2', 'GaCo', 'MnSnRh2', 'ScRu', 'Dy2B4C', 'HfPd3', 'YN', 'MgGaRh2', 'Nb3Ga2', 'HoRh2', 'MgInIr2', 'Nb3Sb', 'MnGaNi2', 'ZnCuNi2', 'Y2Zr2O7', 'TbN', 'TmN', 'NbSbRu', 'Hf2CuOs', 'MgSnRh2', 'SmB6', 'TiNi2Sb', 'Ho(SiRu)2', 'Hf2CoRe', 'ZrPd3', 'ZnGeN2', 'NdPt3', 'LuSnRh2', 'HfAlPt', 'TiSnO4', 'YTaRu2', 'HoB2', 'ScNi2', 'Y2O3', 'Mn2CoSb', 'TbPt2', 'GaN', 'Sc2O3', 'Ti2AlTc', 'HfMgO3', 'MgTiO3', 'Nb3Ge', 'TmB2', 'ScNi4Sn', 'TiCo2Sn', 'ZrCo2Sn', 'MnNi2Sn', 'LuPt3', 'Ho(SiIr)2', 'NbAlO4', 'NbS', 'Sc2Co3Si', 'HfSbRu', 'ZnPd', 'ZrRh', 'TmB6', 'TiMn2Ga', 'ZrMn2', 'Mn2CoGe', 'ZnSnO3', 'LiZrIr2', 'Tm(SiRu)2', 'LiGaRh2', 'ScInIr2', 'NdRhC2', 'Hf2CuIr', 'MnCo2Sn', 'SmBRh3', 'Tm(SiRh)2', 'DyN', 'SmPt2', 'TiNi2Sn', 'Ti2MnGe', 'GaPt', 'Ti2AlMo', 'Ga2O3', 'LiTiRh2', 'LuGaRh2', 'Lu2Fe2Si2C', 'TmPt2', 'SmRu2', 'LiNbRh2', 'HoB6', 'HoNi5', 'Hf2ZnRe', 'HoNi4B', 'LiAl2Ir', 'Ti3Ni4', 'Mg(BeN)2', 'Zr3(CuSi)4', 'DyGaO3', 'ZrZnNi2', 'ZnNi3', 'NbZnO3', 'HfInPt2', 'TbGaO3', 'Zr3AlC2', 'Dy2Zr2O7', 'ZnPd3C', 'SmN', 'LuPt2', 'LiAl2O4', 'Nb3Sn', 'DyPt2', 'Ga2NiRh', 'MgPt2', 'NdNi5', 'TmRh2', 'TbRh2', 'ZrSnRu', 'HfSnRu', 'HoPt2', 'Tm(PRu)2', 'Zr2Co3Si', 'LuRh2', 'Zr3Rh']
```

[{'material': 'Ti3AlC2', 'reason': 'Ti3AlC2 is a MAX phase material known for its excellent corrosion resistance, especially in aggressive environments. The presence of titanium and aluminum makes it suitable for saltwater applications.'}, {'material': 'TiPd', 'reason': 'Titanium-palladium alloys exhibit exceptional corrosion resistance in chloride-rich environments, such as saltwater, due to the formation of a protective oxide layer that prevents degradation.'}, {'material': 'TiAlPd2', 'reason': 'Titanium-aluminum-palladium alloys are used in marine applications due to their high resistance to saltwater corrosion and strong protective oxide formation.'}, {'material': 'Ti2ZnRe', 'reason': 'The combination of titanium, zinc, and rhenium contributes to strong corrosion resistance, especially in chloride environments, making it potentially suitable for saltwater applications.'}, {'material': 'NbInO4', 'reason': 'Niobium-based compounds like NbInO4 are known for high resistance to corrosion in saline environments, as niobium forms stable oxide layers that prevent degradation in chloride media.'}, {'material': 'Hf2CuOs', 'reason': 'Hafnium-copper-osmium alloys have demonstrated stability in corrosive environments, with hafnium contributing to a stable protective oxide layer, suitable for saltwater exposure.'}, {'material': 'Zr3AlC2', 'reason': 'As a MAX phase material containing zirconium, Zr3AlC2 offers strong corrosion resistance, with zirconium forming a robust oxide layer in chloride environments.'}, {'material': 'ZrPd3', 'reason': 'Zirconium-palladium alloys are known for excellent saltwater corrosion resistance, attributed to the formation of protective oxide layers and the noble nature of palladium.'}, {'material': 'Nb3Sn', 'reason': 'Niobium-tin compounds exhibit good corrosion resistance in chloride environments, making them potentially viable for saltwater applications due to the protective oxide films that can form.'}, {'material': 'HfPd3', 'reason': 'Hafnium-palladium alloys are known for excellent corrosion resistance in marine environments, as they form protective oxide layers that resist degradation in chloride-rich media.'}, {'material': 'Ti2TcPd', 'reason': 'This titanium-technetium-palladium alloy is likely to exhibit high corrosion resistance due to the presence of titanium and palladium, which are both resistant to chloride attack in saltwater.'}]

FIG. S5. Conversational records with GPT-4o for corrosion-resistant materials in saltwater environments. Documentation of interactions with GPT-4o to identify materials suitable for corrosion resistance in saltwater applications. The material list includes deduplicated compositions generated by ElaTBot. ElaTBot is responsible for generating materials with corresponding bulk moduli, while GPT-4o is responsible for screening materials that can resist corrosion in saltwater environments.

As a materials expert, please review the provided materials list and identify potential materials suitable for the protective layer of LiCoO2 electrode in lithium batteries. Focus on materials that exhibit structural stability and can accommodate the expansion and contraction of active materials during cycling. Please respond in JSON list format. Each JSON should include the potential materials and the reasons why they might meet the requirements.

```
['Ba2AsAu', 'SrSnHg', 'SmMg3', 'NaErTl2', 'Li3Al', 'Nd3In', 'Sr2AsAu', 'BaCuBi', 'CaMgHg2', 'SmTm3', 'Li2NdIn', 'Ac2SnHg', 'CaMg6W', 'Sr2BiAu', 'SmY3', 'Li2PmTl', 'Ca2SnS4', 'Na2LiNF6',
'Ca3SbN', 'Mg2Hg', 'Sr3(AlGe)2', 'NdTm3', 'CsCaF3', 'Li3In', 'Sm3Er', 'SrS', 'Ca5Si3', 'Sr2SbAu', 'Ac3Sn', 'SrZnSn', 'BaCO3', 'Mg3In', 'Li2NdAl', 'CaAcZn2', 'Pr3Al', 'LiMg6Mo', 'Na3AlF6', 'Ca3SbAs',
'LiCuS', 'Ca2Si', 'Sm3In', 'Ba2SbAu', 'SmMg', 'LiMg2Pd', 'BaLiP', 'Mg3Mn', 'Cs2PdC2', 'CsCdF3', 'Ba3(AlGe)2', 'SrMg6Ti', 'Li3SbS4', 'LiMg2Hg', 'Li2MgSi', 'Tb', 'Sr2Cu(BrO)2', 'Pr3In', 'Ba3In2Br2O5',
'Ca2Cu(BrO)2', 'Li3Ga', 'BaSb3', 'Sm3Al', 'Mg6VB', 'MgCd', 'Tb3TlC', 'BaLiH3', 'Li2PrIn', 'Ac2ZnGe', 'CaPrCd2', 'Pr3Tl', 'BaSn5', 'SrAcZn2', 'CaPrZn2', 'Li2S', 'Cs2PtC2', 'AcMgCd2', 'Li2CdAu',
'CaCdSn', 'CsCu5S3', 'NdMg', 'Li2CaSi', 'Li2CuSb', 'Ba3SnO', 'Tm3AlC', 'Sr3AsN', 'NaPrHg2', 'Mg3Hg', 'NaTmTl2', 'Ba3N2', 'SrMg6Zr', 'Ba(NO3)2', 'LiCdAs', 'Ca3AsCl3', 'Sr2H6Ru', 'Li3Pt', 'Ca3AsP',
'PrYMg2', 'Ac2CdSn', 'Ac2SiHg', 'Ca2CdSn', 'Li2PmIn', 'SrHgPb', 'NdLuMg2', 'Sr3BiN', 'Mg3Bi', 'Ca5(AlSb3)2', 'NdTmMg2', 'PrMg3', 'Ca6Al2NF', 'Li2AgSn', 'Li2AgSb', 'SrMgH4', 'Sm3V', 'Mg6SiB',
'Sr3(AlSn)2', 'Li2AgAu', 'Li2CdPb', 'BaZnGe', 'Ba(MgAs)2', 'NaHoTl2', 'CaCdHg2', 'Ba(MgSb)2', 'Mg3Tl', 'Li2CdGe', 'Sr3(AlGe2)2', 'Ca2BiAu', 'Nd3Tl', 'Li2MgGe', 'LiAc2Si', 'LiTbTl2', 'NdErMg2',
'CaMg6Zr', 'PrErMg2', 'Cs2CaF4', 'LiAc2Ge', 'CaMg6Mo', 'PrMg', 'Ca2ZnRh', 'AcMg3', 'Li2AgPb', 'Tm3TlC', 'NaSmHg2', 'TbMg3', 'Mg3Cd', 'Tm', 'Na2LiN', 'Li2CaGe', 'BaGe2', 'PrDyMg2', 'Ca6In2NF',
'Sm', 'TbMg', 'BaCdGe', 'Ca5Sb3', 'CaPmCd2', 'Li2InAg', 'CaMgCd2', 'Sr2CuBr3', 'Ca2CuSn', 'LiTmTl2', 'Sr2ZnPt', 'Cs2NaTlF6', 'Ca3BiN', 'Ca6MnBi2', 'CaMg6Ti', 'Cs2KTlF6', 'Mg2In', 'Sr2ZnRh',
'Sr2CuBr2O', 'NdMg3', 'SrZnGe', 'Mg2Cd', 'Li2PrSb', 'PrY3', 'SmTmMg2', 'Li2SnSb', 'Sr2ZnRu', 'Li2PrPb', 'TmMg', 'Mg2Mn', 'Nd3Al', 'SrZnHg2', 'Mg2TlCd', 'LiInAg2', 'MgSc2Cd', 'Tm2MgTl',
'LiGaAg2', 'MgSc2Al', 'SmHoZn2', 'Mg2Zn11', 'Pm2ZnHg', 'Ca(AlSi)2', 'Pm2ZnAg', 'LiCd2Pd', 'Ca3SbN', 'Li2PdAu', 'BaAl9Fe2', 'PrInAg2', 'MgCuBi', 'Nd2ZnGa', 'La3InN', 'PrP', 'Tm2MgAl', 'Y2MgAl',
'LaPbAu2', 'YCd', 'BaCO3', 'LaHgAu2', 'Li2InRh', 'CaPmAu2', 'LiAlAg2', 'DyMgHg2', 'Mg2AgAu', 'NdIn3', 'DyYHg2', 'CaSn2Pd', 'Y2ZnIn', 'Li2GaAu', 'Li2SbPd', 'LaInAg2', 'DyCdHg2', 'LiMg2Pd',
'PrSb', 'Mg3Mn', 'Pm2AgGe', 'SrAgP', 'Li2Pt', 'Ca(CdP)2', 'DyYZn2', 'LiPm2Ru', 'Ba2ZnN2', 'Ca3SnO', 'LiAlGe', 'SmTmHg2', 'YCd3', 'Dy2TlAg', 'Ca3N2', 'Sr3GaN3', 'BaGeF6', 'Mg3Au', 'PrTe',
'Li2AlPd', 'Pm2CdSn', 'BaPd2', 'Y2Al', 'Ca3GeO', 'Ca3(AlGe)2', 'Pm2ZnGe', 'BaZnF4', 'SmDyHg2', 'NdAgHg2', 'LiAg2Sn', 'Sm2AgHg', 'Sr(AgGe)2', 'SrAlSiH', 'CaF2', 'Pr2ZnAg', 'SmYZn2', 'SmMgHg2',
'Ca(AgGe)2', 'SmMgAg2', 'Mg2H6Ru', 'SmDyZn2', 'Sm2TlAg', 'Nd2AgHg', 'Ca6MnN5', 'CaZnSi', 'Li3Pt', 'Li2CuGe', 'Li2SbAu', 'Ca3SiO', 'TbCd3', 'Li2CuP', 'TbMgHg2', 'Pr3AlC', 'La2ZnAg',
'SmTmZn2', 'CaZnF4', 'Mg2ZnPd', 'Pr2AgHg', 'Mg3Cu', 'YMgAg2', 'LiZnAg2', 'LiCdAg2', 'YErZn2', 'YMgHg2', 'LiAg2Ge', 'Dy2MgAl', 'Li2InPd', 'TbY3', 'Li2AlAg', 'SmYAl2', 'Sr3(AlSi)2', 'LiPm2Rh',
'Sm2ZnAg', 'Mg2Cu', 'TmCd3', 'Y3InC', 'SrPdF4', 'Sm2ZnHg', 'LaAgHg2', 'LiY2Ru', 'PmCdHg2', 'Pm2CdGe', 'LiPm2Pt', 'LiMgSnAu', 'PrCdHg2', 'LiTbHg2', 'BaCuF4', 'SmLuZn2', 'Li2GaPd', 'NdTeCl',
'LiGaSi', 'Sm2ZnGa', 'YErIn2', 'Y2AlZn', 'Mg3P2', 'Ba(MgP)2', 'YTl3', 'MgAg', 'Ca3GeN', 'LiMg2Rh', 'BaAlGe', 'LiAgF2', 'SrAl4', 'Mg3Co', 'LiZnSnAu', 'YTmZn2', 'Y3Tm', 'YTl', 'TbLuIn2', 'MgAgSn',
'SmYHg2', 'TbTmZn2', 'SmLuHg2', 'NdHoZn2', 'SrAl2(SiO4)2', 'PrAg2Hg', 'Li3GaN', 'BaCu2Ge', 'Pm2AgHg', 'La2ZnHg', 'TbCd', 'TbMgAg2', 'NdZn', 'NdCdHg2', 'CaCdAu2', 'Pm2CdAg', 'TmMgHg2',
'PrPbAu2', 'TmMgCd2', 'DyTlAg2', 'DyMgGa', 'Tb2MgAl', 'Tb2MgTl', 'LiTb2Ru', 'PrAgHg2', 'Tb2CdS4', 'PrHg3', 'PrAgSn', 'SmErZn2', 'NdMgAg2', 'NdZn2Ag', 'LaAgSn', 'SrAlPd', 'LiTm2Ru',
'Tm2MgIn', 'PrMgAg2', 'Dy2ZnIn', 'Y2ZnAg', 'TmAl3', 'NdP', 'PrH2', 'LiGaAg2', 'HoSe', 'Pm2ZnRh', 'ErAl3', 'Pm2AgPt', 'Tm2ZnHg', 'TbS', 'ErCu', 'Ca3GaN3', 'Mg3Ir', 'NdSe2', 'Li2PdAu', 'Ca3CrN3',
'ScZn', 'Pr2AgRu', 'SmP', 'LiAlAg2', 'YAl', 'Mg2AgAu', 'ScAl', 'YGe', 'SmSnAu2', 'LiZn2Pd', 'LiScRu', 'SmGa3', 'YAl2', 'Li2SbPd', 'PrGe3', 'MgCu', 'Sm2AgRu', 'CaPmRh2', 'Y2Zn17', 'Sc2ZnCu',
'TmAs', 'YAl3', 'SmCdAu2', 'LiSc2Te', 'DyAgGe', 'ErAgSn', 'TmGa3', 'Y2AgRu', 'Mg2AgPt', 'Sc2AgHg', 'LiMgPd2', 'DyCu', 'NdGeRu', 'LiCd2Pt', 'LiPm2Ru', 'HoInAg2', 'HoNiBi', 'NdS', 'Sc3SnB',
'Pm2ZnPt', 'MgCuSn', 'TbSe', 'Sc3Al', 'YMgAu2', 'Ca3N2', 'DyH2', 'LiIn2Rh', 'YNiBi', 'Li2AlPd', 'Tm2MgTe', 'MgScAg2', 'HoP', 'ScZn2Ag', 'LiY2Ir', 'LiGaAu2', 'CaNdRh2', 'ErInAg2', 'DyS', 'Sc2AlCd',
'HoCuSn', 'DySe', 'LiMgSnPd', 'Ca4HfN4', 'DyInAu2', 'SmS', 'Sc3InN', 'Pm2ZnRu', 'CaF2', 'Sc2MnSn', 'ScAl3', 'ErZn2', 'TbAs', 'ErH', 'Sc2CdS4', 'LiPm2Ir', 'Sc3TlC', 'Ca6MnN5', 'Tm2ZnAg', 'LiMg2Pt',
'DyAg2', 'Mg2ZnRh', 'Pm2CuPt', 'LiIn2Pt', 'DyP', 'TmCu', 'Er2ZnAu', 'SmH2', 'TbP', 'Sm2ZnRu', 'Li2GaPt', 'ErGa3', 'YCu', 'PrAl2', 'Li2InPt', 'TmZr', 'YCuSn', 'LiZn2Au', 'HoCu', 'TbZrSb', 'Sc2ZnGa',
'Li2GaRh', 'TbCdAg2', 'ScZn3', 'YAgHg2', 'TbGa3', 'YCdAu2', 'MgNiBi', 'PrSiAg', 'HoInCu2', 'LiPm2Rh', 'CaSi2', 'Nd2AgIr', 'Y3InC', 'NdSeF', 'YCdAg2', 'SmInAg2', 'LiY2Ru', 'ErAl2', 'MgCuAs',
'LiPm2Pt', 'Pm2CuRu', 'Y2ZnRu', 'NdSi2', 'Li2InIr', 'Li2GaPd', 'DySb', 'LiGa2Pd', 'HoS', 'Mg3Mo', 'NdSnAu2', 'TbCdAu2', 'LiCdPd2', 'SmInAu2', 'ScCdAg2', 'Sm2ZnIr', 'CaSnPd', 'Y3AlC', 'Sc2MnGe',
'SmAs', 'CaSn2Ir', 'Mg3Rh', 'ScGa3', 'LiMg2Rh', 'Ca3FeN3', 'LiSc2Pt', 'PrNiBi', 'Li2PtAu', 'TbZn5', 'DyAl2', 'Er2ZnAg', 'Er2AgHg', 'YInAg2', 'PrGeAu', 'NdNiBi', 'Pm2AgRu', 'CaSnPd2', 'TmCdAg2',
'SmNiBi', 'MgCu2Sn', 'Dy2AgHg', 'Tb2ZnAu', 'Li2PdRh', 'Tm2ZnAu', 'Nd2AgRu', 'Li2CuPd', 'Tb2ZnRu', 'Tm2MgRu', 'TmZn3', 'Ho2ZnAu', 'Tb2AgHg', 'SmCuPb', 'Dy2ZnAu', 'Sc2CuSn', 'Ca6Si2N5',
'ErCdAg2', 'Y2AgIr', 'ZrAl', 'Ti3Ga', 'ErNiSb', 'Sm2IrRu', 'DyNiSb', 'Ti2Sn', 'ScNiSb', 'ScCu3', 'Zr3Al', 'Ti3Al', 'HoCu4Au', 'TbS', 'Ti2Zn', 'NdNiGe2', 'Li2GaIr', 'Sc2CuRu', 'Ca3CrN3', 'Sc3AlC', 'YSnPd2',
'NdSnRh', 'MgNi', 'ScSnAu', 'HoCu5', 'ZrCdCu2', 'ErCu5', 'CaSn(BO3)2', 'Li2InZn2Rh', 'TmCdPd2', 'NdNi2', 'LiSc2Ru', 'Sc2AlC', 'NdC2', 'MgCu', 'CaPmRh2', 'Sc2AlRu', 'HoFeSi', 'Ti3Sb', 'MgInPd2', 'TiZn',
'Ba(SbO3)2', 'ScSbPt', 'NdFe5', 'Dy2AgIr', 'HoSbPt', 'Y2AgRu', 'LiMgPd2', 'Mg2Cu3Si', 'LiCd2Pt', 'LiGa2Pt', 'Mg2AgRh', 'Hf3Bi', 'Ba2ZrO4', 'NdFeSi2', 'YCu5', 'MgNi2Sb', 'NdS', 'Ca(NiP)2', 'HoCdCu4',
'ZrCu', 'TiGa3', 'LiIn2Rh', 'ScNi', 'HfAl3', 'Mg3Re', 'ZrInAu', 'Y2ZnIr', 'NdPd3', 'HoNiSb', 'LiAl2Pd', 'Sc2CuAu', 'YInCu2', 'TbInAu2', 'DyCu5', 'Zr5Sn4', 'SmSnPt', 'ZrZn3', 'Sc3NiC', 'DyS', 'SmFeSi',
'SmS', 'Ba(BeN)2', 'CaF2', 'YCdPd2', 'HfSb', 'Er2AgIr', 'Tm2AgRu', 'YS', 'Sc3TlC', 'Dy2IrAu', 'LiCu2Ge', 'ZrSTe', 'Y2CuIr', 'Zr2Ag', 'LiZnPd2', 'Tm2ZnIr', 'LiBeN', 'MgCu4Sn', 'Y2CuRu', 'SmFe5', 'ErS',
'HfAl', 'MgSc2Os', 'Zr2Cu', 'Ba(PRh)2', 'Liln2Ir', 'ErBiPt', 'ErCdCu4', 'Mg2PdAu', 'Li2GaRh', 'Ho2AgIr', 'TmSbPt', 'ZrZn', 'LiAl2Ni', 'Sc2CuTe', 'LiBeO3', 'SmNi2', 'Dy2CuOs', 'MgSc2Ru', 'ZrSb', 'Zr3Sn',
'ScNiSn', 'ScCdCu2', 'Nd2IrRh', 'Hf2Al', 'TmCu5', 'TbPd', 'MgSc2Te', 'YNiSb', 'ZrSnPd', 'Ti2AlZn', 'Sc2AlTe', 'HoFe2', 'YInPd2', 'Ti2CuSb3', 'TbNiSb', 'BaTiO3', 'Li2GaPd2', 'ScAgAu', 'ScInAu2', 'HoS',
'ScCdPd2', 'TmNiSb', 'Zr2Al', 'ScInCu2', 'Sm2AgIr', 'YAl2Ni', 'ScSbPd', 'TbNi2', 'MgSnPd2', 'LiSc2Ir', 'Ca2SiO4', 'Hf2Zn', 'Mg2AgIr', 'LiZn2Pt', 'HoPd', 'LiCuO2', 'Ca(SbO3)2', 'ScInCu4', 'TiZn3',
'Ca(AsPd)2', 'Sc2AgRu', 'Ba(BIr)2', 'TmS', 'Zr3Tl', 'TiSb', 'LiZn2Rh', 'MgInCu4', 'HfZn3', 'LiSc2Pt', 'Ba3SnO4', 'YPd', 'SmNiSb', 'Sm2IrAu', 'TmCdCu4', 'Li2NiP2', 'Ba2CuO4', 'MgSnPd', 'Ba2YCuO5',
'Zr2Sn', 'HoCdPd2', 'Tm2CuOs', 'TbCdCu4', 'Ho2AgRu', 'Tm2AgIr', 'Er2AgRu', 'Mg2ZnIr', 'NdCdPd2', 'Ca3(AlNi)4', 'HfSn', 'TiCdAu2', 'Er2CuIr', 'Ho2IrAu', 'TbCdPd2', 'Zr3Ga', 'Hf3Sn', 'NdSnPd2',
'Zr3Sb', 'Hfln3', 'Y3AlN', 'TiSn', 'BaNi2Sn', 'HfCuSn', 'ZrCuSn', 'SmCdPd2', 'Er2CuOs', 'Li2CuPd', 'SmSnPd2', 'Nd2IrRu', 'Tm2CuRu', 'BaNi2Sb', 'Nd2CuOs', 'Ho2CuOs', 'TbCu4Au', 'HfInCu2', 'Ti3Ga',
'Sm2IrRu', 'TmCdRh2', 'Zr3Al', 'Ti3Al', 'HoCu4Au', 'Nd(SiPd)2', 'HoPd3', 'Zr2SnC', 'Sc2NiIr', 'TiSnPd', 'ZrInAu2', 'LuPd3', 'MgScRh2', 'Ti3Sn', 'ZrS', 'ZrP', 'YPd3', 'Hf2CuSb3', 'YOF', 'Zr3Cu', 'Sc2TcAu',
'ScSnPt', 'Y2O3', 'Ti3Sb', 'MgInPd2', 'TiNiSn', 'TiZn', 'MnSbRh', 'ZrSnPt', 'YSnO3', 'TiZnAu2', 'Al3Pd2', 'MgNi2Sn', 'LuCdRh2', 'LiGa2Pt', 'Mg2PdRh', 'Y(CoGe)2', 'ZrAlCu2', 'LiGa2Ir', 'Sc2AlOs',
'TiZnCu2', 'LuNi2Sn', 'TiAlCu2', 'HfMgAu2', 'HfAl3', 'Ti2AlCr', 'NdPd3', 'LiAl2Pd', 'Mg2PtRh', 'Sc2TcAg', 'Sc2AgIr', 'NdOF', 'Hf3(Cu2Ge)2', 'TmPd3', 'YNiP', 'ScInPd2', 'HfZn', 'Y2IrRh', 'ZrAlAu2',
'LiAl2Rh', 'Zr2Pd', 'Lu2CoRu', 'AlCrCu2', 'HoNi2', 'LiNi2Ge', 'Al2Pd', 'HfInAu2', 'LiBePd2', 'Y2CuIr', 'TiCu', 'LiZnPd2', 'Tm2ZnIr', 'LiBeN', 'Sm2IrRh', 'AlCu3', 'LiZr2Os', 'Sm(CoSi)2', 'Zr2Cu',
'Ti2AlCu', 'LiAl2Pt', 'MnP4', 'Nd(CoSi)2', 'TiCuSn', 'HfZnAu2', 'Sc2CuOs', 'Ti2Cu', 'LiIn2Ir', 'Hf3Sb', 'ZrCu5', 'TiAlAu2', 'Zr3P', 'ScCuPd2', 'LiNbO3', 'Sm2O3', 'ScCdRh2', 'Sc2AgOs', 'SmNi2', 'Zr3Sn',
'ZrZnCu2', 'Zr3Ga2', 'MgZrPd2', 'YCuO2', 'Nd2IrRh', 'MnCoTe', 'Ti3Au', 'TmSnRh', 'Hf2Al', 'Sc2CoRu', 'Zr2AlC', 'Ho2OsAu', 'AlCuAu2', 'ZrSnPd', 'MnCoSb', 'ZrInCu2', 'LiZr2Ir', 'MgInRh2', 'ScCdPd2',
'ScSnPd2', 'MnSnPd2', 'Lu2IrRu', 'SmRh', 'Mg2SiO4', 'Ti2MnAl', 'HfAlCu2', 'Hf2Zn', 'LiAl2Ir', 'Ti2AlV', 'Ti2AlC', 'ScInCu4', 'TmS', 'LiInRh2', 'ScNi2Sn', 'Ho(CoGe)2', 'SmPd3', 'LiZn2Pt', 'NdO3',
'Tm2IrRu', 'MgSnPt', 'NdRh2', 'YCdRh2', 'Tm2IrRh', 'HoCdRh2', 'Nd(CoGe)2', 'LiZnRh2', 'Ti2ZnCu', 'Ti2ZnNi', 'Hf3Al', 'TmNi2', 'ZrZnAu2', 'LiGaPd2', 'Tb(CoGe)2', 'TiCdAu2', 'Sc2NiRu', 'LiCe2Ir',
'HoSnRh2', 'Sc2CoTe', 'Hf3Sn', 'Zr2NiSn', 'HfCuSn', 'TbCdRh2', 'LuSnPd2', 'Nd2IrRu', 'MgSnRh', 'Y2IrRu', 'LiCu2Pd', 'Tb2IrRu', 'Hf2Sb', 'Lu2RuAu']
```

```
[{'material': 'Li2S', 'reasons': ['Common in sulfide-based solid electrolytes and interfacial coatings', 'Can mitigate side reactions and buffer volume changes at the cathode', 'Stable
interface in some all-solid-state battery concepts', 'Often forms stable interfaces with oxide cathodes (if processed appropriately)']}, {'material': 'Li3SbS4', 'reasons': ['Known
sulfide-type solid electrolyte (superionic conductor)', 'Often investigated for thin coating layers on cathodes', 'Flexible and can help accommodate cathode volume changes']},
{'material': 'Na2LiNF6', 'reasons': ['Complex lithium-containing fluoride', 'Can serve as a stable passivation layer to inhibit side reactions', 'Potential to provide a mechanically
robust interface']}, {'material': 'CaF2', 'reasons': ['Chemically inert, stable fluoride commonly used as a protective coating', 'Very high structural stability though negligible Li-ion
conductivity (acceptable if ultra-thin)', 'Often used in vacuum/electronics contexts to prevent unwanted surface reactions']}, {'material': 'Mg2SiO4', 'reasons': ['Forsterite-
structured magnesium silicate with high thermal and chemical stability', 'Oxide-based layers are known to improve interface durability in batteries', 'Relatively rigid lattice but
can help mitigate mechanical stress at the cathode interface']}, {'material': 'BaTiO3', 'reasons': ['Well-known perovskite oxide with good structural stability', 'Chemically robust
and can be deposited as a thin film', 'Helps prevent direct contact between the electrolyte and active cathode material']}, {'material': 'Ti2AlC', 'reasons': ['Representative MAX
phase (ceramic–metal hybrid) known for toughness and damage tolerance', 'Capable of withstanding mechanical stress from electrode expansion/contraction', 'Thermally and
chemically stable under typical battery fabrication conditions']}, {'material': 'LiNbO3', 'reasons': ['One of the most commonly studied protective coatings on LiCoO2 and other
cathodes', 'Exhibits good chemical stability and compatibility at higher potentials (~4 V)', 'Known to reduce side reactions and improve cycle life by buffering volume changes']},
{'material': 'Ca2SnS4', 'reasons': ['Potentially stable sulfide phase at moderate voltages', 'Could serve as an inert barrier if deposited thinly']}, {'material': 'TbS', 'reasons': ['Rare-
earth sulfide with high lattice energy', 'Likely chemically stable under inert conditions (though untested in Li-ion cells)']}, {'material': 'SmS', 'reasons': ['Another rare-earth
monosulfide with strong bonding', 'Potentially an inert barrier at the cathode interface']}, {'material': 'DyS', 'reasons': ['Rare-earth sulfide possessing high melting point', 'Could be
stable if not oxidized at high potential']}, {'material': 'Cs2NaTlF6', 'reasons': ['Structurally stable mixed fluoride', 'In theory can passivate LiCoO2 (though Tl toxicity is a major
practical barrier)']}, {'material': 'Cs2KTlF6', 'reasons': ['Similar to Cs2NaTlF6 in composition and stability', 'Contains toxic thallium, so not truly viable in real batteries']},
{'material': 'Cs2CaF4', 'reasons': ['Layered alkaline/alkali fluoride that might remain stable at 4+ V', 'No direct battery data but plausible as a thin passivating film']}, {'material':
'BaZnF4', 'reasons': ['Complex fluoride known for chemical stability', 'Potential protective/passivating layer if it adheres well', 'Likely an electrical insulator, so must be ultra-
thin']}, {'material': 'CaZnF4', 'reasons': ['Same structural family as BaZnF4, with Ca substituting Ba', 'Chemically stable in dry conditions; no direct Li-battery data']}, {'material':
'BaGeF6', 'reasons': ['A barium–germanium fluoride complex', 'High-temperature and chemical stability in inert atmospheres', 'Could isolate the cathode surface if thinly
deposited']}, {'material': 'BaCuF4', 'reasons': ['Another complex fluoride with moderate thermal stability', 'May serve as a robust surface film if not oxidized', 'Unexplored in
LiCoO2 contexts but plausible by analogy']}, {'material': 'SrPdF4', 'reasons': ['Mixed Pd–fluoride with potential chemical inertness', 'Costly composition, but stable if well-
formed', 'No battery-specific data; a theoretical coating candidate']}, {'material': 'CaSn(BO3)2', 'reasons': ['Calcium–tin borate, likely stable in dry, high-temperature conditions',
'Potentially inert to typical cathode operating voltages', 'Hypothetical but structurally robust']}, {'material': 'SrAl2(SiO4)2', 'reasons': ['Strontium aluminosilicate with strong
network bonding', 'Expected inertness in many chemical environments', 'Deposition as a thin layer would be needed for battery use']}, {'material': 'Ca3SiO', 'reasons':
['Uncommon calcium–silicon–oxygen compound', 'Potential stability under moderate voltages', 'Mechanical properties and actual inertness need verification']}, {'material':
'Ca3GeO', 'reasons': ['Similar to Ca3SiO but with Ge substitution', 'May offer robust structural stability in an oxygen matrix', 'No confirmed battery data']}, {'material': 'Ba3SnO',
'reasons': ['Barium–tin oxide, fairly high-temperature stability', 'Could passivate LiCoO2 if not electrochemically decomposed', 'Must be applied as an ultra-thin film']},
{'material': 'Ca3SbN', 'reasons': ['Alkaline-earth pnictide nitride with high structural stability', 'Could be inert at battery-relevant voltages (untested)', 'Might suppress side
reactions if stable']}, {'material': 'Ca3BiN', 'reasons': ['Bismuth-containing analog of Ca3SbN', 'Likely a robust lattice structure', 'No direct data in Li-ion systems']}, {'material':
'Sr3AsN', 'reasons': ['Strontium-based pnictide nitride', 'Could be refractory and inert under certain conditions', 'Must confirm no redox instability at ~4 V vs. Li']}, {'material':
'Sr3BiN', 'reasons': ['Bismuth version of Sr3AsN', 'Potential chemical stability if not oxidized', 'Hypothetical passivation layer']}, {'material': 'Ca6Al2NF', 'reasons': ['Mixed
nitride-fluoride system with possible partial ionic conduction', 'Chemically stable under certain conditions', 'Requires specialized synthesis and testing']}, {'material': 'Ca6MnN5',
'reasons': ['Complex nitridomanganate, often high melting and stable', 'Potential mechanical hardness for protective layering', 'Electrochemical inertness unverified']}, {'material':
'Ca3GeN', 'reasons': ['Calcium–germanium nitride with robust crystal framework', 'Unknown battery performance, but plausible inertness']}, {'material': 'Ca3CrN3', 'reasons':
['Chromium nitride network, known for hardness', 'Could handle mechanical stress from electrode cycling', 'Possible oxidation risk at high voltage—needs vetting']}, {'material':
'Ca3FeN3', 'reasons': ['Iron-based nitridometalate, stable at high temperatures', 'Might be chemically inert in a sealed cell', 'No published Li-ion data']}, {'material': 'Sc3InN',
'reasons': ['Transition-metal nitride with possible refractory properties', 'Stable in inert atmospheres, hypothetical for LiCoO2', 'No direct testing so far']}, {'material': 'Y3AlN',
'reasons': ['Yttrium–aluminum nitride variant, typically high melting point', 'Often inert in electronics packaging contexts', 'Could be a protective passivation if thin']}, {'material':
'Ca3N2', 'reasons': ['Calcium nitride stable in moisture-free conditions', 'Potentially inert in sealed Li-ion cells', 'Requires verification of voltage stability']}, {'material': 'Sc2AlC /
Sc3AlC', 'reasons': ['MAX-phase–like compounds with ceramic-metal characteristics', 'High fracture toughness and thermal stability', 'Could buffer mechanical stress at the
cathode surface']}, {'material': 'Li3GaN', 'reasons': ['Lithium-containing gallium nitride (hypothetical compound)', 'Might allow Li-ion conduction if it forms a stable phase', 'No
known data in battery usage']}, {'material': 'LiAgF2', 'reasons': ['Lithium–silver fluoride, possibly stable vs. oxidation', 'Could passivate the surface if no undesired redox occurs',
'Needs thorough electrochemical tests']}, {'material': 'LiBeN', 'reasons': ['Lithium beryllium nitride—likely stable in principle', 'Severe toxicity concerns around Be', 'Purely
theoretical for battery coatings']}, {'material': 'Ba3N2', 'reasons': ['Barium nitride with high lattice energy', 'Sensitive to moisture but might remain stable in sealed conditions',
'Unclear electrochemical window']}, {'material': 'SrAlPd', 'reasons': ['Intermetallic that can be highly corrosion-resistant', 'Could form an inert barrier if it does not oxidize at high
voltage', 'No direct battery data; purely hypothetical']}, {'material': 'Ba(MgP)2', 'reasons': ['Barium magnesium phosphide, high melting point', 'Potentially strong covalent
framework', 'Risk of oxidation to phosphates at high voltage']}, {'material': 'Ca(NiP)2', 'reasons': ['Calcium nickel phosphide, similarly robust network', 'Phosphides can be stable
if not oxidized', 'Again, untested in Li-ion cells, so purely theoretical']}]
```

FIG. S6. Conversational records with GPT-4o for the lithium battery electrode protective layers materials discovery. Documentation of interactions with GPT-4o to identify the protective layers materials that could be used in $LiCoO_2$ electrode. The material list provided consists of deduplicated compositions generated by ElaTBot. ElaTBot is responsible for generating materials with corresponding bulk moduli, while GPT-4o is responsible for screening materials that meet users' requirements.

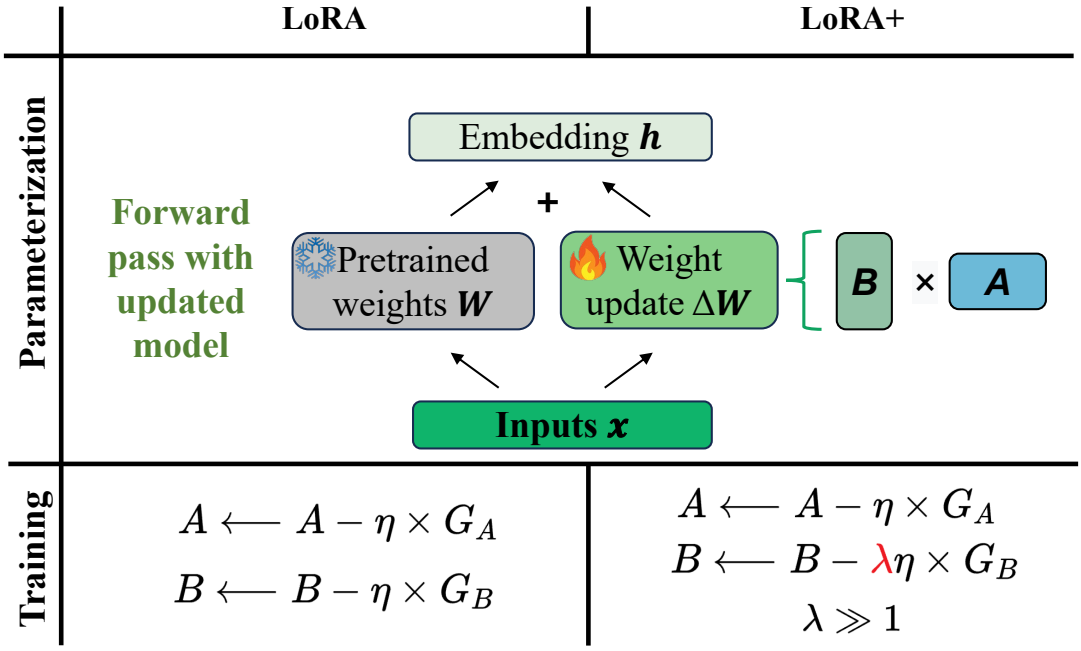


FIG. S7. Parameter Efficient Fine-tuning (PEFT) methods: LoRA (Low-Rank Adaptation) and LoRA+.

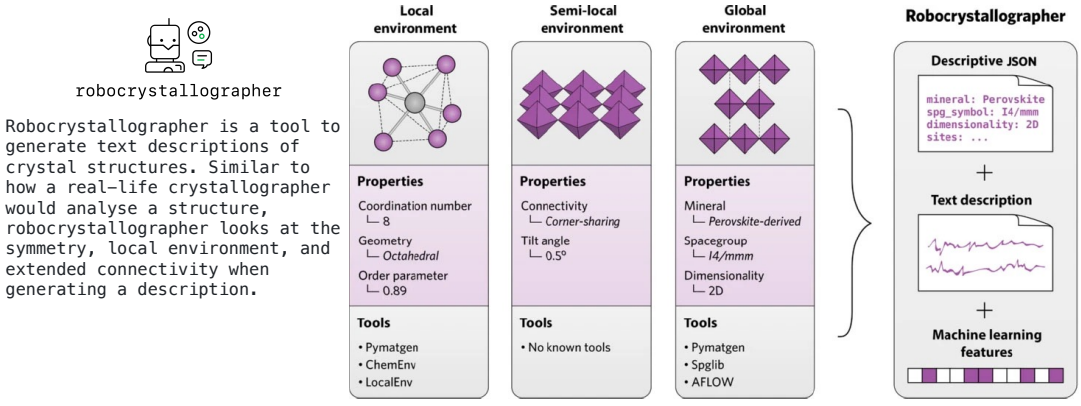


FIG. S8. Methods we used to generate structure textual description.

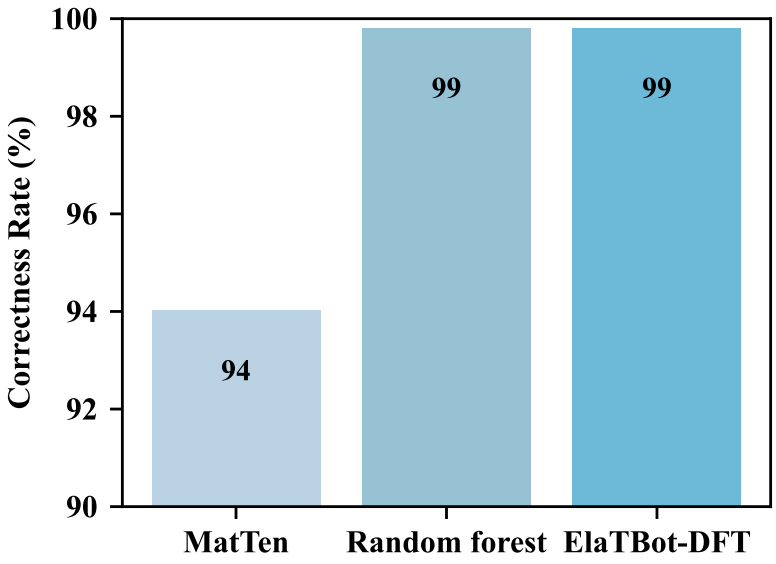


FIG. S9. Stability test of elastic constant tensors of three models on the test set. For the 519 materials in the test set, 518 are found to be elastically stable for predictions of both the random forest model and our ElaTBot-DFT model, whereas the predictions of MatTen failed the stability test in 32 cases.

# 3 Supplementary Tables

TABLE S1. Evaluation of prompt variants for training ElaTBot-DFT. Various text-based prompts were tested during training with Llama2-7b to determine optimal performance. Textual descriptions generated from each prompt were compared to other methods, leading to the selection of the most effective prompt for constructing ElaTBot-DFT.

| Prompt Type | Prompt Template |
|---|---|
| 1. System Instruction + Structure JSON Information | Given a material's symmetry and conventional cell structure, predict the elastic tensor of it directly and accurately with scientific logic. Answer without any other comments, descriptions, or explanations. The answer should be a $6 \times 6$ Python matrix. The material information is presented in JSON format. Information JSON of Material TiB2:{'material_formula': 'TiB2', 'symmetry': {'crystal_system': 'Hexagonal', 'symbol': 'P6/mmm', 'number': 191, 'point_group': '6/mmm', 'symprec': 0.1}, 'conventional_structure': {'lattice': {'matrix': [[1.517019, -2.627554, 0.0], [1.517019, 2.627554, 0.0], [0.0, 0.0, 3.227438]], 'a': 3.034038, 'b': 3.034038, 'c': 3.227438, 'alpha': 90.0, 'beta': 90.0, 'gamma': 120.0, 'volume': 25.729454}, 'sites': [{'species': [{'element': 'Ti', 'occu': 1}], 'xyz': [0.0, 0.0, 0.0]}, {'species': [{'element': 'B', 'occu': 1}], 'xyz': [1.517019, -0.875851, 1.613719]}, {'species': [{'element': 'B', 'occu': 1}], 'xyz': [1.517019, 0.875851, 1.613719]}]}} |
| 2. System Instruction + Structure Description | Given a material's crystal structure description, predict the elastic constant tensor of it directly and accurately with scientific logic. Answer without any other comments, descriptions, or explanations. The answer should be a $6 \times 6$ Python matrix. TiB2 is hexagonal omega structure structured and crystallizes in the hexagonal P6/mmm space group. Ti(1) is bonded to twelve equivalent B(1) atoms to form a mixture of face and edge-sharing TiB12 cuboctahedra. All Ti(1)-B(1) bond lengths are 2.38 Å. B(1) is bonded in a 9-coordinate geometry to six equivalent Ti(1) and three equivalent B(1) atoms. All B(1)-B(1) bond lengths are 1.75 Å. |
| 3. System Instruction + Composition Description | Given a material's composition description, predict the elastic constant tensor of it directly and accurately with scientific logic. Answer without any other comments, descriptions, or explanations. The answer should be a $6 \times 6$ Python matrix. The material TiB2 with a reduced composition of {'Ti': 1.0, 'B': 2.0} exhibits a density of 4.485 $g/cm^3$ and a density per atom of 8.576 $g/cm^3$. The information about the elements contained in the material is as follows. B has an electronegativity of 2.04, an ionization energy of 8.298 eV, a bulk modulus of 320.0 GPa, an atomic radius of 0.87 Å. Ti has an electronegativity of 1.54, an ionization energy of 6.828 eV, a bulk modulus of 110.0 GPa, a Young's modulus of 116.0 GPa, a Poisson's ratio of 0.32, an atomic radius of 1.76 Å. |
| 4. System Instruction + Composition Description + Structure Description **(we finally use this to train ElaTBot-DFT!)** | Given a material description, predict the elastic constant tensor of it directly and accurately with scientific logic. Answer without any other comments, descriptions, or explanations. The answer should be a $6 \times 6$ Python matrix. The material TiB2 with a reduced composition of {'Ti': 1.0, 'B': 2.0} exhibits a density of 4.485 $g/cm^3$ and a density per atom of 8.576 $g/cm^3$. The information about the elements contained in the material is as follows. B has an electronegativity of 2.04, an ionization energy of 8.298 eV, a bulk modulus of 320.0 GPa, an atomic radius of 0.87 Å. Ti has an electronegativity of 1.54, an ionization energy of 6.828 eV, a bulk modulus of 110.0 GPa, a Young's modulus of 116.0 GPa, a Poisson's ratio of 0.32, an atomic radius of 1.76 Å. TiB2 is hexagonal omega structure structured and crystallizes in the hexagonal P6/mmm space group. Ti(1) is bonded to twelve equivalent B(1) atoms to form a mixture of face and edge-sharing TiB12 cuboctahedra. All Ti(1)-B(1) bond lengths are 2.38 Å. B(1) is bonded in a 9-coordinate geometry to six equivalent Ti(1) and three equivalent B(1) atoms. All B(1)-B(1) bond lengths are 1.75 Å. |

TABLE S2. Performance comparison among different prompts on the same test set.

| Prompt Type | Bulk modulus MAE (GPa) | $R^2$ | $\overline{C_{ij}}$ MAE (GPa) | $R^2$ |
|---|---|---|---|---|
| 1 | 9.04 | 0.947 | 2.79 | 0.947 |
| 2 | 8.12 | 0.955 | 2.45 | 0.957 |
| 3 | 8.60 | 0.954 | 2.67 | 0.956 |
| 4 | 7.74 | 0.963 | 2.32 | 0.965 |

TABLE S3. Performance comparison with previous algorithms on the same test set (0K). 0 K training set was used because MatTen requires the structural information at 0 K.

| Algorithm | Bulk modulus MAE(GPa) | $R^2$ | $\overline{C_{ij}}$ MAE(GPa) | $R^2$ |
|---|---|---|---|---|
| Random forest | 10.58 | 0.927 | 3.33 | 0.924 |
| MatTen | 7.98 | 0.959 | 2.43 | 0.963 |
| Darwin (Llama2-based) | 11.35 | 0.918 | 3.47 | 0.915 |
| This work (Llama2 with prompt4) | 7.74 | 0.963 | 2.32 | 0.965 |

TABLE S4. Different tasks and prompt templates for training ElaTBot in knowledge fusion training stage.

| Task | Prompt Template |
|---|---|
| elastic constant tensor prediction task | Given a material description, predict its elastic constant tensor at 0K temperature accurately and directly using scientific logic. Provide the answer as a $6 \times 6$ Python matrix without additional comments, descriptions, or explanations. The material TiB2 with a reduced composition of 'Ti': 1.0, 'B': 2.0 exhibits a density of 4.485 $g/cm^3$ and a density per atom of 8.576 $g/cm^3$. The information about the elements contained in the material is as follows. B has an electronegativity of 2.04, an ionization energy of 8.298 eV, a bulk modulus of 320.0 GPa, an atomic radius of 0.87 Å. Ti has an electronegativity of 1.54, an ionization energy of 6.828 eV, a bulk modulus of 110.0 GPa, a Young's modulus of 116.0 GPa, a Poisson's ratio of 0.32, an atomic radius of 1.76 Å. TiB2 is hexagonal omega structure structured and crystallizes in the hexagonal P6/mmm space group. Ti(1) is bonded to twelve equivalent B(1) atoms to form a mixture of face and edge-sharing TiB12 cuboctahedra. All Ti(1)-B(1) bond lengths are 2.38 Å. B(1) is bonded in a 9-coordinate geometry to six equivalent Ti(1) and three equivalent B(1) atoms. All B(1)-B(1) bond lengths are 1.75 Å. |
| Bulk modulus prediction task | Given a material description, predict its Voigt bulk modulus (unit: GPa) at 0K temperature accurately and directly using scientific logic. Provide the answer in the form of individual numerical value without additional comments, descriptions, or explanations. The material TiB2 with a reduced composition of 'Ti': 1.0, 'B': 2.0 exhibits a density of 4.485 $g/cm^3$ and a density per atom of 8.576 $g/cm^3$. The information about the elements contained in the material is as follows. B has an electronegativity of 2.04, an ionization energy of 8.298 eV, a bulk modulus of 320.0 GPa, an atomic radius of 0.87Å. Ti has an electronegativity of 1.54, an ionization energy of 6.828 eV, a bulk modulus of 110.0 GPa, a Young's modulus of 116.0 GPa, a Poisson's ratio of 0.32, an atomic radius of 1.76 Å. TiB2 is hexagonal omega structure structured and crystallizes in the hexagonal P6/mmm space group. Ti(1) is bonded to twelve equivalent B(1) atoms to form a mixture of face and edge-sharing TiB12 cuboctahedra. All Ti(1)-B(1) bond lengths are 2.38 Å. B(1) is bonded in a 9-coordinate geometry to six equivalent Ti(1) and three equivalent B(1) atoms. All B(1)-B(1) bond lengths are 1.75 Å. |
| Material generation task | Generate a material chemical formula and its crystal system with a Voigt bulk modulus of 256.56 GPa at a temperature of 0K. Use scientific reasoning step-by-step and directly output the answer without additional comments, descriptions, or explanations. |
| Infilling task | Below is a partial description of a material where the chemical formula has been replaced with the string '[MASK]'. The material is [MASK] with a reduced composition of 'Ti': 1.0, 'B': 2.0. Generate the chemical formula that could replace [MASK]. |

TABLE S5. Prediction results of ElaTBot with/without RAG. To ensure a fair comparison, we used the prompt "What's the Voigt bulk modulus of <crystal system> <composition> at <temperature number>?" To minimize irrelevant content generation when querying without RAG, we included an additional instruction: "Just provide the result". This template is intentionally simple and differs from the fine-tuning template to isolate the impact of RAG and reduce the influence of other factors. It is important to note that RAG performance depends on factors like the embedding model and recall method. Here, we present a basic application using the Hugging Face free embedding model 'intfloat/multilingual-e5-large'.

| Materials | Temperature (K) | Experimental Bulk Modulus (GPa) | Predicted Bulk Modulus With RAG (GPa) | Predicted Bulk Modulus W/O RAG (GPa) |
|---|---|---|---|---|
| $Ni_3Al$ | 113 | 173.93 | 171.83 | Output Error |
| $Ni_3Al$ | 162 | 173.03 | 172.83 | 133.33 |
| $Ni_3Al$ | 223 | 172.3 | 170.1 | 105.31 |
| $\gamma^{'} - PE16$ | 113 | 178.53 | 175.33 | Output Error |
| $\gamma^{'} - PE16$ | 162 | 177.8 | 176.37 | 109.33 |
| $\gamma^{'} - PE16$ | 223 | 177.13 | 173.83 | 108.33 |
| $\gamma - TiAl$ | 170 | 111.35 | 111.31 | 108.33 |
| $\gamma - TiAl$ | 230 | 110.91 | 110.77 | 108.3 |
| $\gamma - TiAl$ | 270 | 110.41 | 109.83 | 108.31 |

TABLE S6. Elastic constant tensors prediction performance of different crystal systems on the ElaTBot-DFT test set.

| Crystal System | Count | MAE (GPa) | $R^2$ |
|---|---|---|---|
| Cubic | 208 | 2.0291 | 0.9740 |
| Tetragonal | 101 | 2.3790 | 0.9555 |
| Hexagonal | 73 | 2.0483 | 0.9688 |
| Orthorhombic | 69 | 3.0048 | 0.9413 |
| Trigonal | 40 | 2.5931 | 0.9620 |
| Monoclinic | 28 | 2.9683 | 0.9335 |
| Triclinic | 3 | 2.0556 | -3.0961 |

TABLE S7. Bulk modulus prediction performance of different crystal systems on the ElaTBot-DFT test set.

| Crystal System | Count | MAE (GPa) | $R^2$ |
|---|---|---|---|
| Cubic | 208 | 7.0225 | 0.9720 |
| Tetragonal | 101 | 7.7359 | 0.9610 |
| Hexagonal | 73 | 7.0792 | 0.9570 |
| Orthorhombic | 69 | 9.3511 | 0.9452 |
| Trigonal | 40 | 8.7556 | 0.9627 |
| Monoclinic | 28 | 9.8373 | 0.9382 |
| Triclinic | 3 | 3.7037 | 0.2819 |

TABLE S8. RAG sensitivity test results. Comparison of predictions based on knowledge base with 37 (Type 1) and 28 (Type 2) data points.

| Materials | Temperature (K) | Experimental Bulk Modulus (GPa) | Type 1 | Type 2 |
|---|---|---|---|---|
| $Ni_3Al$ | 113 | 173.93 | 172.87 | 171.83 |
| $Ni_3Al$ | 162 | 173.03 | 173.03 | 172.83 |
| $Ni_3Al$ | 223 | 172.3 | 172.3 | 170.1 |
| $\gamma^{'} - PE16$ | 113 | 178.53 | 175.53 | 175.33 |
| $\gamma^{'} - PE16$ | 162 | 177.8 | 175.33 | 176.37 |
| $\gamma^{'} - PE16$ | 223 | 177.13 | 177.13 | 173.83 |
| $\gamma - TiAl$ | 170 | 111.35 | 111.39 | 111.31 |
| $\gamma - TiAl$ | 230 | 110.91 | 110.91 | 110.77 |
| $\gamma - TiAl$ | 270 | 110.41 | 110.41 | 109.83 |